

Synthesis and characterization of $\text{Li}_{1/3}\text{Ce}_{2/3}\text{PO}_4$ and $\text{LiCe}_{2/3}\text{PO}_4$ ceramics

This article has been downloaded from IOPscience. Please scroll down to see the full text article.

2007 J. Phys.: Condens. Matter 19 106204

(<http://iopscience.iop.org/0953-8984/19/10/106204>)

View [the table of contents for this issue](#), or go to the [journal homepage](#) for more

Download details:

IP Address: 129.252.86.83

The article was downloaded on 28/05/2010 at 16:29

Please note that [terms and conditions apply](#).

Synthesis and characterization of $\text{Li}_{1/3}\text{Ce}_{2/3}\text{PO}_4$ and $\text{LiCe}_{2/3}\text{PO}_4$ ceramics

T Salkus^{1,5}, A Kezionis¹, A Dindune², Z Kanepė², J Ronis², J Miskinis³,
V Kazlauskienė³, L J Gauckler⁴, U P Mücke⁴ and A F Orliukas¹

¹ Faculty of Physics, Vilnius University, Sauletekio aleja 9/3, LT-10222 Vilnius, Lithuania

² Institute of Inorganic Chemistry, Riga Technical University, LV-2169 Salaspils, Latvia

³ Institute of Materials Science and Applied Research, Vilnius University, Sauletekio aleja 9/3, LT-10222 Vilnius, Lithuania

⁴ ETH Zurich, Department Materials, Nonmetallic Inorganic Materials, Wolfgang-Pauli-Street 10, CH-8093 Zurich, Switzerland

E-mail: tomas.salkus@ff.vu.lt

Received 5 September 2006, in final form 13 December 2006

Published 15 February 2007

Online at stacks.iop.org/JPhysCM/19/106204

Abstract

$\text{Li}_{1/3}\text{Ce}_{2/3}\text{PO}_4$ and $\text{LiCe}_{2/3}\text{PO}_4$ compounds were synthesized by a solid state reaction and studied by x-ray diffraction and thermogravimetric analysis. At room temperature the investigated compounds exhibit monoclinic symmetry (space group $P2_1/n$) with four formula units in the lattice. The compounds are stable up to 1200 K in air and show no weight loss. The ceramic samples were fabricated with varying sintering times. The surfaces of the ceramics were studied by scanning electron microscopy. The increase of sintering time of the ceramics leads to an increase of the grain size of the materials. The results of an x-ray photoelectron spectroscopy study have shown that the external electric field changes the Li amount on the surfaces of the ceramic samples. The electric properties of the samples were investigated by complex impedance spectroscopy in the frequency range from 50 to 1.2×10^9 Hz in the temperature range from 300 to 650 K. Varying the sintering time of the ceramics affects the values of the total conductivity, activation energy, dielectric permittivity and dielectric losses of the ceramics.

1. Introduction

Solids with high ionic conductivity are essential materials for the development of high energy batteries [1] and sensitive CO_2 sensors [2]. These materials have LISICON- or NASICON-type network structures [3, 4]. It is known that $\text{Li}_3\text{Sc}_2(\text{Fe}_2)(\text{PO}_4)_3$ polycrystals and single crystals are solid electrolytes with fast Li^+ ion transport [5–7].

⁵ Author to whom any correspondence should be addressed.

Esaka *et al* reported that the addition of Li ions in the YPO_4 compound caused the appearance of the ionic conductivity of $\text{Li}_{3x}\text{Y}_{1-x}\text{PO}_4$ solid solution [8]. Orlova *et al* synthesized $\text{LiCe}_2(\text{PO}_4)_3$ and $\text{Li}_3\text{Ce}_{1.5}(\text{PO}_4)_3$ compounds by the liquid-phase method and studied them by x-ray diffraction at room and elevated temperatures [9]. They reported that in $\text{LiCe}_2(\text{PO}_4)_3$ and $\text{Li}_3\text{Ce}_{1.5}(\text{PO}_4)_3$ cerium exists as Ce(IV) and Ce(III) respectively.

The above-mentioned compounds have typical CePO_4 monazite-type structure and exhibit monoclinic symmetry (space group $P2_1/n$) with four formula units in the lattice [9]. The thermal expansion coefficients along particular crystal axes of $\text{LiCe}_2(\text{PO}_4)_3$ compound are anisotropic, and were found to be $\alpha_a = 7.73 \times 10^{-6} \text{ deg}^{-1}$, $\alpha_b = 6.44 \times 10^{-6} \text{ deg}^{-1}$, and $\alpha_c = 7.73 \times 10^{-6} \text{ deg}^{-1}$ [9]. According to [10], the relative density, grain size and thermal expansion coefficient of monazite ceramics depend on the sintering temperature and sintering time. The authors of [11] reported that monazite crystals synthesized by a hydrothermal method at 373 and 473 K exhibit hexagonal and monoclinic symmetry respectively. X-ray photoelectron spectroscopy (XPS) indicated that the phosphorus exists completely in the form of PO_4^{3-} and cerium exists as Ce(III), with no Ce(IV) in any crystal [11]. We found no information in the literature about the investigation of electric properties and XPS of monazite doped by Li^+ ions.

In the present paper we report the technological conditions for the synthesis of $\text{Li}_{1/3}\text{Ce}_{2/3}\text{PO}_4$ and $\text{LiCe}_{2/3}\text{PO}_4$ powder, sintering of the ceramic samples and the results of our investigations of x-ray diffraction (XRD) from the powder, thermo-gravimetric analysis (TGA), x-ray photoelectron spectroscopy (XPS), scanning electron microscopy (SEM), and electrical properties of the ceramics in the frequency range from 50 to 1.2×10^9 Hz in the temperature range from 300 to 650 K.

2. Experimental details

Powders of $\text{Li}_{1/3}\text{Ce}_{2/3}\text{PO}_4$ and $\text{LiCe}_{2/3}\text{PO}_4$ have been synthesized from a mixture of Li_2CO_3 (99.999%), CeO_2 and $\text{NH}_4\text{H}_2\text{PO}_4$ (extra pure) by solid-state reaction. The powder was milled in a planetary mill for 12 h using ethyl alcohol as milling fluid with one milling ball of 52 mm in diameter. After the milling the mixture was heated at 723 K for 3 h and then milled again for 12 h. The $\text{Li}_{1/3}\text{Ce}_{2/3}\text{PO}_4$ powder was heated at 1173 K for 1 h in air and after milling was kept at the same temperature for a further 3 h. The $\text{LiCe}_{2/3}\text{PO}_4$ powder was heated at 1123 K for 4 h. After heating the $\text{Li}_{1/3}\text{Ce}_{2/3}\text{PO}_4$ and $\text{LiCe}_{2/3}\text{PO}_4$ powders were milled for 8 h. The fine powders, with an average particle size of 0.1 μm , were dried at 393 K for 24 h.

The structure parameters of $\text{Li}_{1/3}\text{Ce}_{2/3}\text{PO}_4$ and $\text{LiCe}_{2/3}\text{PO}_4$ were obtained at room temperature from x-ray powder diffraction patterns using $\text{Cu K}\alpha_1$ radiation. The scanning rate in the 2Θ range from 6° to 80° was 1° min^{-1} . The thermal stability of the obtained compounds was studied in a TGA system (STA 449 C, NETZSCH). The heating rate was 10 K min^{-1} .

$\text{Li}_{1/3}\text{Ce}_{2/3}\text{PO}_4$ and $\text{LiCe}_{2/3}\text{PO}_4$ powders were uniaxially cold pressed at 300 MPa. The ceramics were sintered in air for 1, 2, and 3 h. The sintering temperatures of $\text{Li}_{1/3}\text{Ce}_{2/3}\text{PO}_4$ and $\text{LiCe}_{2/3}\text{PO}_4$ ceramic samples were 1083 and 1163 K respectively. XPS was used to identify the valence states of Ce and elemental compositions of the ceramics. All XPS measurements were recorded by excitation with x-rays with $h\nu = 1253.6 \text{ eV}$. The pressure in the XPS chamber was 10^{-8} Pa .

Platinum electrodes were prepared on a $\text{LiCe}_{2/3}\text{PO}_4$ ceramic cylindrical sample (8 mm diameter, 1 mm thick) by applying a conductive Pt paste fired at 900 K. The first electrode covered the bottom surface of the pellet, and the second electrode had a shape of a ring, was placed on the top surface, and was connected to the negative potential. The ceramic sample

Table 1. X-ray powder diffraction data (Miller indices, diffraction angles, interplanar distances, relative intensities) for the $\text{Li}_{1/3}\text{Ce}_{2/3}\text{PO}_4$ compound at room temperature.

<i>hkl</i>	2Θ	<i>d</i> (Å)	<i>I</i> / <i>I</i> ₀ (%)
−1 0 1	17.05	5.20	5
1 1 0	18.42	4.81	10
0 1 1	18.93	4.69	16
−1 1 1	21.23	4.18	32
1 0 1	21.63	4.105	16
1 1 1	25.12	3.542	16
0 2 0	25.35	3.511	21
2 0 0	26.95	3.306	74
1 2 0	28.77	3.101	100
2 1 0	29.88	2.9879	21
0 1 2; −1 1 2	31.15	2.8699	68
−2 0 2	34.45	2.6013	16
−2 1 2	36.85	2.4372	16
2 2 0	37.35	2.4057	5
0 3 1	41.11	2.1939	26
−3 1 1	42.16	2.1417	52
2 2 1	42.37	2.1315	26
2 1 2	46.05	1.9694	26
3 0 1	46.75	1.9415	10
−2 3 1	47.85	1.8994	21
1 0 3; −1 3 2	48.47	1.8766	42
0 2 3	50.67	1.8001	10
−3 2 2	51.78	1.7641	16
1 3 2	52.43	1.7438	21
1 4 0	54.05	1.6953	16

was placed in the XPS chamber and evacuated. Then an external permanent electric field (E) was applied to the sample and it was heated at 493 K for 1 h. Then the sample under electric field was cooled down to room temperature. The surface of the sample which was under the negative electrode was studied by XPS without an external permanent electric field.

The surfaces of the ceramics were polished using a suspension with 1 μm diamond particles, thermally etched for 1.5 h at 900 K with 10°min^{-1} heating and cooling rates, and studied by SEM. The measurements of complex conductivity ($\tilde{\sigma} = \sigma' + i\sigma''$), complex impedance ($\tilde{Z} = Z' + iZ''$) and complex dielectric permittivity ($\tilde{\epsilon} = \epsilon' - i\epsilon''$) were performed in the temperature range from 300 to 650 K in the frequency range from 50 to 10^6 Hz using an LCR meter (HP 4284A) and in the frequency range from 10^6 to 1.2×10^9 Hz by using a coaxial impedance spectrometer set-up [12].

3. Results and discussion

The x-ray diffraction data of the investigated powder are listed in tables 1 and 2. The lattice parameters and densities of the materials are presented in table 3.

From the results of the x-ray diffraction study we conclude that $\text{Li}_{1/3}\text{Ce}_{2/3}\text{PO}_4$ and $\text{LiCe}_{2/3}\text{PO}_4$ compounds exhibit monoclinic symmetry (space group $P2_1/n$). Both compounds have four formula units in the lattice. The decrease of Li number in the lattice leads to the decreases of the values of density and volume of lattice of the investigated compounds. The results of the x-ray diffraction study of $\text{LiCe}_{2/3}\text{PO}_4$ compound have shown an admixture of Li_3PO_4 of about 7 wt%.

Table 2. X-ray powder diffraction data for the $\text{LiCe}_{2/3}\text{PO}_4$ compound at room temperature.

<i>hkl</i>	2Θ	<i>d</i> (Å)	<i>I</i> / <i>I</i> ₀ (%)
−1 0 1	17.05	5.20	8
1 1 0	18.41	4.81	6
0 1 1	18.93	4.69	14
−1 1 1	21.25	4.18	4
1 0 1	21.67	4.098	17
1 1 1	25.10	3.545	14
0 2 0	25.34	3.512	17
2 0 0	26.98	3.302	64
−1 0 2	28.42	3.138	6
1 2 0	28.77	3.101	100
2 1 0	29.87	2.9889	17
−2 1 1	30.28	2.9493	3
−1 1 2	31.17	2.8671	75
−2 0 2	34.47	2.5998	17
1 1 2	36.65	2.4500	11
−2 1 2	36.85	2.4372	17
2 2 0	37.34	2.4063	7
0 2 2	38.40	2.3423	4
−3 0 1	40.10	2.2468	3
0 3 1	41.12	2.1934	19
−3 1 1	42.15	2.1422	28
2 2 1	42.40	2.1301	17
2 1 2	46.03	1.9702	28
3 0 1	46.70	1.9435	6
2 3 0	47.57	1.9100	3
−2 3 1	47.84	1.8998	11
−1 3 2	48.49	1.8759	22
3 2 0	48.76	1.8661	17
−1 2 3	49.70	1.8330	3
0 2 3	50.67	1.8001	8
−3 2 2	51.78	1.7641	17
1 3 2	52.44	1.7435	18
−2 2 3	52.80	1.7324	8
1 4 0	54.00	1.6967	10
4 0 0	55.60	1.6516	6

Table 3. Lattice parameters and densities of the $\text{Li}_{1/3}\text{Ce}_{2/3}\text{PO}_4$ and $\text{LiCe}_{2/3}\text{PO}_4$ compounds at room temperature.

Compound	<i>a</i> (Å)	<i>b</i> (Å)	<i>c</i> (Å)	β (deg)	<i>V</i> (Å ³)	<i>d</i> _{XRD} (g cm ^{−3})
$\text{Li}_{1/3}\text{Ce}_{2/3}\text{PO}_4$	6.7932(10)	7.0198(11)	6.4685(17)	103.455(17)	299.99	4.23
$\text{LiCe}_{2/3}\text{PO}_4$	6.7961(9)	7.0216(13)	6.4686(14)	103.449(15)	300.21	4.33

The TGA study of the $\text{Li}_{1/3}\text{Ce}_{2/3}\text{PO}_4$ and $\text{LiCe}_{2/3}\text{PO}_4$ powders has shown that these compounds are very stable up to 1200 K (figure 1) in air. The minor mass loss of 0.25% in the $\text{Li}_{1/3}\text{Ce}_{2/3}\text{PO}_4$ powder at about 550 K can be related to adsorbed water.

The XPS spectra of the investigated compounds at room temperature are shown in figures 2(a)–(d). To exclude any effects on the values of binding energies due to charging of the sample during the XPS analysis, all data were corrected by a linear shift such that

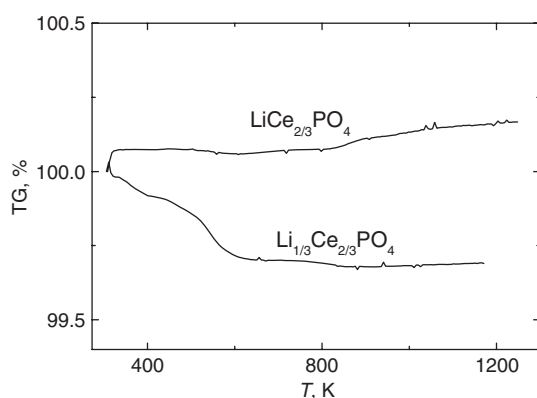


Figure 1. Dependence of mass change of $\text{Li}_{1/3}\text{Ce}_{2/3}\text{PO}_4$ and $\text{LiCe}_{2/3}\text{PO}_4$ powder on temperature while heating.

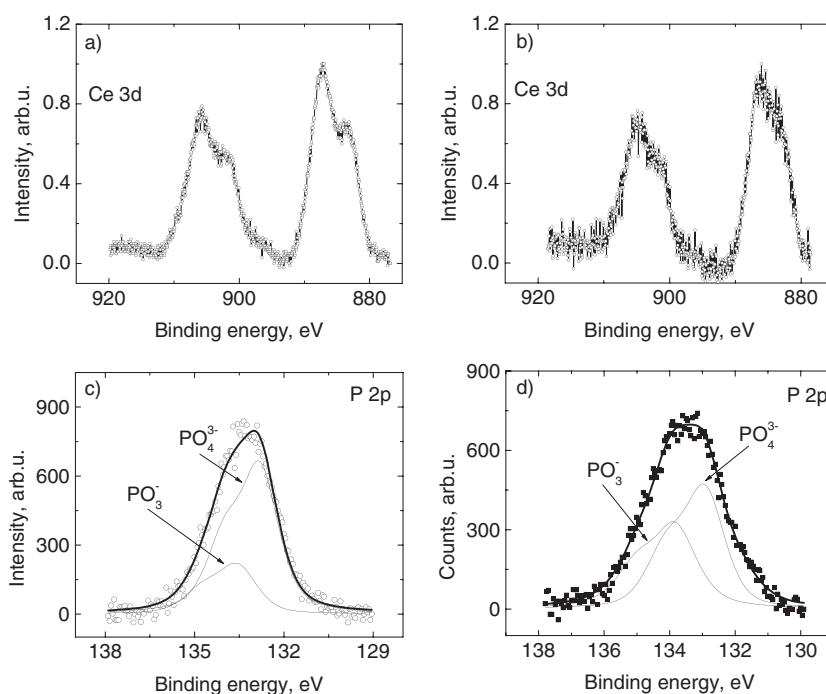


Figure 2. XPS analysis results of $\text{Li}_{1/3}\text{Ce}_{2/3}\text{PO}_4$ Ce 3d (a), $\text{LiCe}_{2/3}\text{PO}_4$ Ce 3d (b), $\text{Li}_{1/3}\text{Ce}_{2/3}\text{PO}_4$ P 2p (c), and $\text{LiCe}_{2/3}\text{PO}_4$ P 2p (d).

the peak maximum of the C 1s binding energy of adventitious carbon corresponded to 284.6 eV.

The Ce 3d spectrum is complex owing to a satellite structure that results from hybridization with the O 2p orbital and partial occupancy of the 4f levels. The Ce 3d spectrum excites a number of components attributed to $3d_{5/2}$ and $3d_{3/2}$ photoelectrons which causes satellite peaks of 'shake-down' type. The peaks at the binding energies of 882.0, 900.5, 888.6, 907.3, 891.8, and 916.4 eV have been assigned to Ce $3d_{5/2}$ and $3d_{3/2}$ characteristic peaks corresponding to

Table 4. The elemental compositions of $\text{Li}_{1/3}\text{Ce}_{2/3}\text{PO}_4$ and $\text{LiCe}_{2/3}\text{PO}_4$ compounds.

Compounds	Atomic %			
	Ce	O	P	Li
$\text{Li}_{1/3}\text{Ce}_{2/3}\text{PO}_4$	9.2	65.8	15.8	9.2
$\text{LiCe}_{2/3}\text{PO}_4$	9.5	59.9	16.5	14.1

Table 5. The comparison of elemental composition of the $\text{LiCe}_{2/3}\text{PO}_4$ compound before and after the influence of E .

	Atomic %			
	Ce	O	P	Li
Before heating in electric field E	9.5	59.9	16.5	14.1
After heating in electric field E	7.1	50.7	18.4	23.8

the Ce^{4+} state [13–16]. Only two doublets have been found in the spectra of Ce 3d if cerium is in the Ce^{3+} state. The Ce 3d_{5/2} spectrum exhibits the two-line structure with peaks at the binding energies 881.6 and 885.5 eV [17, 18], 881.5 and 886 eV [19], 882 and 887 eV [20]. Our result do not show any peak at energies 900.5 and (916–917) eV, which are maximum intensity in the spectra of Ce 3d if cerium is in the Ce^{4+} state. The spectra of Ce 3d in figures 2(a), (b) show the two-line structure with Ce 3d_{5/2} peaks at binding energies ~ 882.3 and ~ 886.2 eV. So we can presume cerium as Ce^{3+} in both investigated compounds. The spectra of P 2p are asymmetric. This indicates that the phosphorus exists in the radical groups PO_4^{3-} and PO_3^- . The binding energy of P 2p photoelectrons is higher when phosphorus is in the radical group PO_3^- compared to PO_4^{3-} [21–23]. The spectra of P 2p were deconvoluted into two components with P 2p_{3/2} binding energies 133.0 eV (PO_4^{3-}) and 133.7 eV (PO_3^-). The P 2p spectra and results of curve fitting are shown in figures 2(c), (d). The elemental compositions of the compounds are summarized in table 4. The comparison of elemental compositions of the studied compounds has shown that an increase of Li content leads to a decrease of the ratio O/P in the compound.

XPS spectra of the $\text{LiCe}_{2/3}\text{PO}_4$ ceramic sample before and after effect of electric field are presented in figures 3(a)–(c). The spectra for Li 1s, P 2p, and O 1s are presented on the y axis with actual counts, i.e. experimental results after the background (Shirley background) has been subtracted.

The intensity of the Li 1s XPS spectra is higher and it is shifted towards lower binding energies. The intensities of the XPS spectra of P 2p and O 1s are lower and they are shifted towards higher binding energies; this shifting indicates an increase of the number of radical groups PO_3^- on the surface. The increase of Li on the studied surface clearly shows that $\text{LiCe}_{2/3}\text{PO}_4$ compound is a Li ion conductor. The results of elemental composition before and after the influence of E are summarized in table 5.

The densities of the ceramics sintered for 1, 2, and 3 h were found to be from 88% to 92% of the theoretical density of the compounds.

After thermal etching, the surfaces of the ceramics were studied by SEM. The SEM images of surfaces of $\text{Li}_{1/3}\text{Ce}_{2/3}\text{PO}_4$ and $\text{LiCe}_{2/3}\text{PO}_4$ ceramics sintered for different sintering time (t_s) are shown in figures 4(a)–(d).

The increase of t_s caused an increase of the size of the ceramic grains. In the SEM images (figures 4(c), (d)) the Li_3PO_4 phase of the ceramic samples can be seen as dark grains.

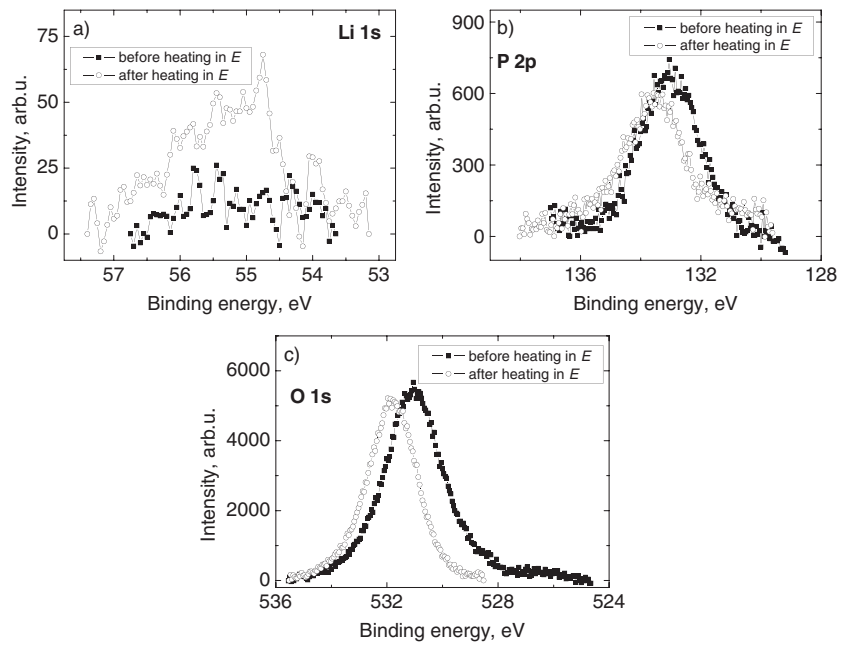


Figure 3. XPS analysis results of $\text{LiCe}_{2/3}\text{PO}_4$ ceramics before and after the influence of E : (a) Li 1s spectrum; (b) P 2p spectrum; (c) O 1s spectrum.

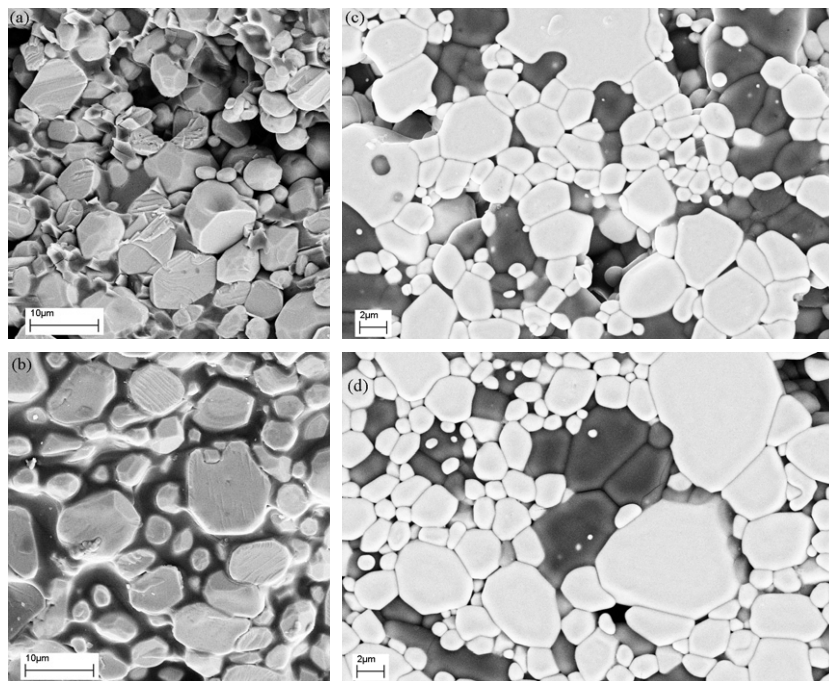


Figure 4. SEM images of $\text{Li}_{1/3}\text{Ce}_{2/3}\text{PO}_4$ ceramics sintered for 1 h (a) and 3 h (b) and $\text{LiCe}_{2/3}\text{PO}_4$ ceramics sintered for 1 h (c) and 3 h (d).

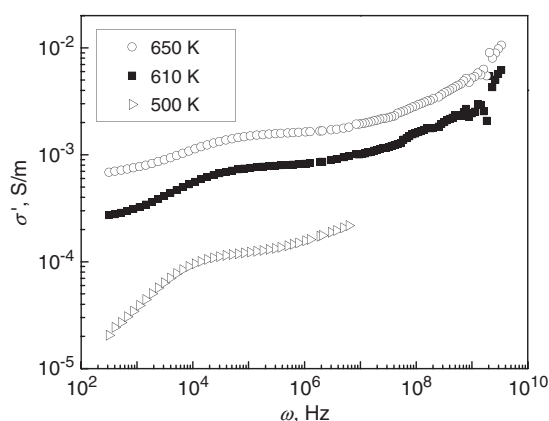


Figure 5. Frequency dependences of the real part of the complex conductivity measured at different temperatures of $\text{Li}_{1/3}\text{Ce}_{2/3}\text{PO}_4$ ceramics sintered for 1 h at 1083 K.

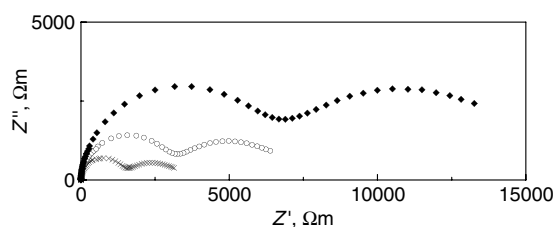


Figure 6. Complex impedance plots measured at temperatures 560 K (\blacklozenge), 600 K (\circ), and 640 K (\times) of $\text{LiCe}_{2/3}\text{PO}_4$ ceramics sintered for 3 h at 1163 K.

The characteristic frequency dependences of the real part of $\tilde{\sigma}$ measured at different temperatures of $\text{LiCe}_{2/3}\text{PO}_4$ ceramics sintered for 3 h at 1163 K are shown in figure 5.

Two dispersion regions were found in the σ' spectra for both investigated samples. The high-frequency part of the obtained spectra may be attributed to the relaxation in grain boundaries, while the lower-frequency part corresponds to processes related to interfaces between the Pt electrodes and the superionic material. The dispersion related to ionic processes in grains is usually observed at high frequencies and temperatures up to about 500 K [12, 24–26]. In our case this dispersion region was not measured due to the low ionic conductivity of the investigated ceramics.

Both processes are thermally activated and the dispersions shift toward higher frequencies with increasing temperature. The temperature dependences of the total (σ_t) conductivities of $\text{Li}_{1/3}\text{Ce}_{2/3}\text{PO}_4$ and $\text{LiCe}_{2/3}\text{PO}_4$ ceramics sintered for different t_s were derived from the complex plots of $\tilde{Z}(\omega)$ and $\tilde{\sigma}(\omega)$ measured at different temperatures. The characteristic complex impedance and complex conductivity plots of the $\text{LiCe}_{2/3}\text{PO}_4$ ceramic sample sintered for 3 h at 1163 K are shown in figures 6 and 7.

The temperature dependences of σ_t of the ceramic samples for different sintering times are shown in figure 8.

The activation energies of the total (ΔE_t) conductivities were found from the slopes of the Arrhenius plots. Different sintering time of the ion conductive ceramics mainly affects the amount of grain boundaries due to grain growth and consequently their contribution to the

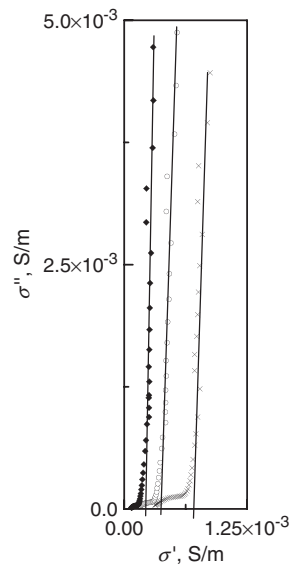


Figure 7. Complex conductivity plots measured at temperatures 560 K (\blacklozenge), 600 K (O), and 640 K (\times) of $\text{LiCe}_{2/3}\text{PO}_4$ ceramics sintered for 3 h at 1163 K.

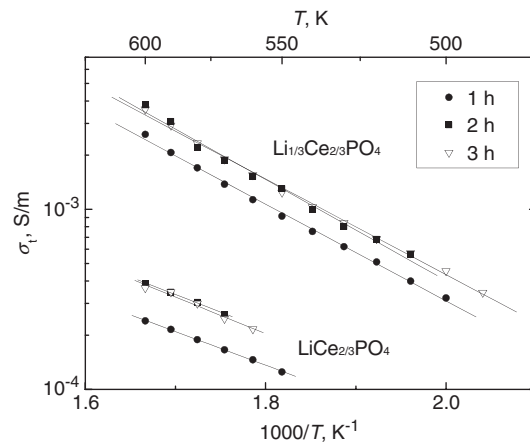


Figure 8. Temperature dependences of total conductivity of $\text{Li}_{1/3}\text{Ce}_{2/3}\text{PO}_4$ and $\text{LiCe}_{2/3}\text{PO}_4$ ceramics with different t_s .

electrical conductivity [12, 24, 25, 27]. The results of the measurements of electrical parameters at 600 K for $\text{Li}_{1/3}\text{Ce}_{2/3}\text{PO}_4$ and $\text{LiCe}_{2/3}\text{PO}_4$ ceramics sintered for different t_s are presented in table 6.

The temperature dependences of the real part of the complex dielectric permittivity and dielectric losses ($\tan \delta$) were investigated at the frequency of 1 GHz. This frequency is higher than the Maxwell relaxation frequency $f_M = \sigma' / 2\pi \epsilon_0 \epsilon'$ (where $\epsilon_0 = 8.85 \times 10^{-12} \text{ F m}^{-1}$ is the dielectric constant of a vacuum). At $T = 600 \text{ K}$, f_M is lower than 110 MHz. The values of ϵ' and $\tan \delta$ of $\text{Li}_{1/3}\text{Ce}_{2/3}\text{PO}_4$ and $\text{LiCe}_{2/3}\text{PO}_4$ compounds sintered for 1, 2, and 3 h at $T = 450 \text{ K}$ are presented in table 7.

Table 6. The results of the measurements of σ_t and ΔE_t at 600 K of $\text{Li}_{1/3}\text{Ce}_{2/3}\text{PO}_4$ and $\text{LiCe}_{2/3}\text{PO}_4$ ceramic samples sintered for different times.

Compounds t_s (h)	$\text{Li}_{1/3}\text{Ce}_{2/3}\text{PO}_4$		$\text{LiCe}_{2/3}\text{PO}_4$	
	σ_t (S m^{-1})	ΔE_t (eV)	σ_t (S m^{-1})	ΔE_t (eV)
1	2.61×10^{-3}	0.54	2.4×10^{-4}	0.37
2	3.8×10^{-3}	0.56	3.87×10^{-4}	0.39
3	3.6×10^{-3}	0.53	3.66×10^{-4}	0.41

Table 7. The results of the measurements of ε' and $\tan \delta$ at 450 K of $\text{Li}_{1/3}\text{Ce}_{2/3}\text{PO}_4$ and $\text{LiCe}_{2/3}\text{PO}_4$ ceramic samples sintered for different times.

Compounds t_s (h)	$\text{Li}_{1/3}\text{Ce}_{2/3}\text{PO}_4$		$\text{LiCe}_{2/3}\text{PO}_4$	
	ε'	$\tan \delta$	ε'	$\tan \delta$
1	7.1	0.076	8.4	0.050
2	6.5	0.037	10.0	0.115
3	8.1	0.051	9.6	0.034

The values of ε' and $\tan \delta$ were found to be independent of temperature in the temperature range from 300 to 500 K. The value of ε' can be affected by the contribution of the migration polarization, vibration of the lattice and electronic polarization.

4. Conclusions

The solid electrolytes $\text{Li}_{1/3}\text{Ce}_{2/3}\text{PO}_4$ and $\text{LiCe}_{2/3}\text{PO}_4$ have been synthesized by solid phase reactions and studied by x-ray powder diffraction. The compounds exhibit monoclinic symmetry (space group $P2_1/n$) with $Z = 4$ formula units in the lattice. The investigated compounds are thermally stable up to 1200 K. The $\text{Li}_{1/3}\text{Ce}_{2/3}\text{PO}_4$ and $\text{LiCe}_{2/3}\text{PO}_4$ ceramics were sintered for 1, 2, and 3 h at 1083 and 1163 K respectively. XPS showed that Ce exists as Ce(III) in both compounds and P was found in the radical group of PO_4^{3-} . The influence of a permanent electric field on the elemental content of the $\text{LiCe}_{2/3}\text{PO}_4$ compound was investigated by XPS. The results of the XPS study have shown that this material can be a Li^+ ion conductor. The ceramics were investigated by complex impedance spectroscopy in the frequency range from 50 to 1.2×10^9 Hz in the temperature range from 300 to 650 K. The sintering time of the ceramics affects the values of the total conductivity, activation energy and densities of the materials. The values of ε' at frequency 1 GHz are related mainly to the polarization process due to the migration of Li^+ ions, lattice vibrations and electronic polarization.

References

- [1] Broussely M, Planchot J P, Rigobert G, Vireu D and Sarre G 1997 *J. Power Sources* **68** 8
- [2] Salam F and Weppner W 1999 *Ionic* **5** 355
- [3] Hong H Y-P 1978 *Mater. Res. Bull.* **13** 117
- [4] Goodenough J B, Hong H Y-P and Kafalas J A 1976 *Mater. Res. Bull.* **1** 203
- [5] Bykov A B, Chirkin A P, Demyanets C N, Doronin S N, Genkina E A, Ivanov-Shits A K, Kondratyuk I P, Maksimov B A, Melnikov O K, Muzodyan L N, Simonov V I and Timofeeva V A 1990 *Solid State Ion.* **3** 31
- [6] Sigarov S, Terziev V G and Dorman J L 1994 *Phys. Rev. B* **49** 6319
- [7] Orliukas A, Vaitkus R, Kežionis A and Aukselis S 1994 *Solid State Ion.* **40/41** 158

- [8] Esaka T, Kobayashi Y, Obata H and Iwahara H 1989 *Solid State Ion.* **34** 287
- [9] Orlova A I, Kitaev D B, Kazantsev N G, Samoilov S G, Kurazhkovskaya V S and Vopilina E N 2002 *Radiochemistry* **44** 326
- [10] Hikichi Y, Nomura T, Tanimura Y and Suzuki S 1990 *J. Am. Ceram. Soc.* **73** 3594
- [11] Zhang Y and Guan H 2003 *J. Cryst. Growth* **256** 156
- [12] Sobiestianskas R, Dindune A, Kanepe Z, Ronis J, Kežionis A, Kazakevičius E and Orliukas A 2000 *Mater. Sci. Eng. B* **76** 184
- [13] Verma A, Bakhshi A K and Agnihotry S A 2006 *Sol. Energy Mater. Sol. Cells* **90** 1640
- [14] Kobayashi Y and Fujiwara Y 2006 *J. Alloys Compounds* **408–412** 1157
- [15] Zhang F, Wang P, Koberstein J, Khalid S and Chan S-W 2004 *Surf. Sci.* **563** 74
- [16] Henderson M A, Perkins C L, Engelhard M H, Thevuthasan S and Peden C H F 2003 *Surf. Sci.* **526** 1
- [17] Pidol L, Viana B, Kahn-Harari A, Galtayries A, Bessière A and Dorenbos P 2004 *J. Appl. Phys.* **95** 7731
- [18] Sameshima S, Hirata Y and Ehira Y 2006 *J. Alloys Compounds* **408–412** 628
- [19] Lee H G, Lee D, Kim S, Kim S G and Hwang C 2005 *Appl. Surf. Sci.* **252** 1202
- [20] Sameshima S, Hirata Y and Ehira Y 2006 *J. Alloys Compounds* **408–412** 628
- [21] Chowdari B V R, Tan K L and Ling F 1998 *Solid State Ion.* **107** 89
- [22] Sherwood P M A 1998 *Surf. Sci. Spectra* **5** 1
- [23] Bertrand P A 1981 *J. Vac. Sci. Technol.* **18** 28
- [24] Godickemeier M, Michel B, Orliukas A, Bohac P, Sasaki K and Gauckler L 1994 *J. Mater. Res.* **9** 1228
- [25] Liu Y and Lao L E 2006 *Solid State Ion.* **177** 159
- [26] Perez-Coll D, Nunez P, Abrantes J C C, Fagg D P, Kharton V V and Frade J R 2005 *Solid State Ion.* **176** 2799
- [27] Orliukas A, Dindune A, Kanepe Z, Ronis J, Kazakevičius E and Kežionis A 2003 *Solid State Ion.* **157** 177